반도체디스플레이기술학회지 제9권 제3호(2010년 9월)
Journal of the Semiconductor & Display Technology, Vol. 9, No. 3. September 2010.

A Numerical Analysis of Polymer Flow in Thermal Nanoimprint Lithography

Nam Woong Kim, Kug Weon Kim*† and Woo-Young Lee**

School of Mechanical Engineering, Dongyang Mirae University, Seoul 152-714, Korea
†*Dept. of Mechanical Engineering, Soonchunhyang University, Asan 336-745, Korea
**School of Mechanical Engineering, Korea University of Technology and Education, Cheonan 330-708, Korea

ABSTRACT

Nanoimprint lithography (NIL) is an emerging technology enabling cost effective and high throughput nanofabrication. To successfully imprint a nanometer scale patterns, the understanding of the mechanism in nanoimprint forming is essential. In this paper, a numerical analysis of polymer flow in thermal NIL was performed. First, a finite element model of the periodic mold structure with prescribed boundary conditions was established. Then, the volume of fluid (VOF) and grid deformation method were utilized to calculate the free surfaces of the polymer flow based on an Eulerian grid system. From the simulation, the velocity fields and the imprinting pressure for constant imprinting velocity in thermal NIL were obtained. The velocity field is significant because it can directly describe the mode of the polymer deformation, which is the key role to determine the mechanism of nanoimprint forming. Effects of different mold shapes and various thicknesses of polymer resist were also investigated.

Key Words : Nanoimprint Lithography, Numerical Analysis, Polymer Flow

1. Introduction

Nanoimprint lithography (NIL) is a promising technology for the fabrication of nanometer scale patterns with low cost, high throughput and high resolution [1,2]. A typical process of NIL is that a mold with nanostructures on its surface is pressed against a substrate and coated with a resist material, to replicate patterns by physical or chemical methods. Among many different types of NIL, the thermal NIL is the earliest and most mature one. Thermal NIL sets the thermal cycle to heat up the imprinted resist polymer over its glass transition temperature, while the high pressure is preserved during the hot embossing procedure.

A few studies investigated the filling behavior of NIL that treated polymer as either an elastic solid material [3,4], a viscoelastic solid [5], a viscous Newtonian fluid [6-8] or even a viscoplastic material [9,10] in simulations. Using a fluid model in simulations, the numerical results can describe the polymer deformation and velocity fields of fluid simultaneously. The study of the velocity fields is significant because the velocity field can directly describe the mode of the polymer deformation, which is the key role to determine the mechanism of nanoimprint forming.

Through numerical simulations, this paper reports the effects of mold shapes and initial resist thickness on polymer flow field during thermal NIL. The variations of cavity width and initial polymer resist thickness are considered as the parameters. By using the commercial finite element analysis code ANSYS, simulations were performed for fluid flow of thermal NIL. To simplify the simulation and reduce the computing time, a single unit cell of the regular pattern mold was utilized and only half of the two-dimensional unit cell was analyzed due to a symmetric model. For a simulating filling behavior, an unsteady incompressible flow with free surfaces was solved on an Eulerian grid to track the deforming interface between the polymer resist and mold by using the volume of fluid (VOF) and grid deformation methods.

†E-mail : kimkug1@sch.ac.kr

2. Numerical Simulation Method

An empirically determined optimal temperature of NIL is 70-80°C above the glass transition temperature, T_g, of the polymer material used [2]. In this temperature range, the elastic effect of the polymer almost disappears and the viscous effect dominates. Therefore, in this range, the polymer is assumed to be a viscous fluid. If we additionally assume an isothermal process, the polymer viscosity can be described by a truncated power law model,

$$\eta(\dot{\gamma}) = \begin{cases} \eta_0 & , \ \dot{\gamma} < \dot{\gamma}_0 \\ \eta_0(\dot{\gamma}/\dot{\gamma}_0) & , \ \dot{\gamma} > \dot{\gamma}_0 \end{cases} \quad (1)$$

where, h, $\dot{\gamma}$, $\dot{\gamma}_0$, and h_0 are viscosity, shear strain rate, limit shear strain rate, and zero shear viscosity, respectively. If $\dot{\gamma}$ is less than $\dot{\gamma}_0$, the viscosity is assumed to be constant (this constant value is called the zero shear viscosity). If $\dot{\gamma}$ is greater than $\dot{\gamma}_0$, the viscosity decreases by the shear thinning effect which follows a power law. In many practical applications, the maximum value of the shear strain rate during the NIL process is less than the limit shear rate, so the viscosity can be regarded to have zero shear viscosity [11]. The PMMA, with viscosity 10^4 Pa·s and density 1.19 g/cm^3 was utilized in the simulation.

If the cross-sectional shape of the mold is constant in one direction, as in the line-and-space pattern as shown in Fig. 1, two-dimensional analysis is possible. Moreover, if the teeth and the cavity of the mold are regular and symmetric, we can use a unit cell of the (two-dimensional) patterned mold as an analysis model by taking into account repeated symmetric boundary conditions. As illustrated in Figs. 1 and 2, H denotes the initial polymer resist thickness, $2W$ and C correspond to the width and height of the cavity of the repeated pattern, respectively, and $2S$ is the width of the mold teeth of the repeated pattern. By ignoring the dynamic effects, the polymer flow was commonly viewed as an incompressible flow. To simplify the analysis, the mold was assumed to be isothermal and rigid, the imprinting velocity was constant, and the air pressure of the cavity was ignored. The computation domain and the associated boundary conditions of the simulation are schematically shown in Fig. 2 where *(f)* represents non-slip boundary conditions and *(s)* indicates symmetric boundary conditions. Geometry parameters such as duty ratio and thickness ratio and the performance index, filling ratio, were defined as follows;

- Duty ratio: the ratio of cavity width to mold pattern width
- Thickness ratio: the ratio of cavity height to initial polymer resist thickness
- Filling ratio: the ratio of polymer filling volume to cavity volume

or

$$\mathrm{DR} = \mathrm{DR} = \frac{W}{W+S} \quad (2)$$

$$\mathrm{TR} = \frac{H}{C} \quad (3)$$

$$\mathrm{FR} = \frac{V \cdot t \cdot (W+S)}{W \cdot C} \quad (4)$$

where V: imprinting velocity
t: imprinting time

The fluid element of ANSYS was employed to model the polymer flow during imprinting process. The 4 node 141 fluid element was implemented to represent the polymer flow. VOF (Volume of Flow) and ALE (Arbitrary Lagrange and Euler Method) of solution conditional options were activated in this simulation. In a VOF analysis, ANSYS uses an advection algorithm for the volume fraction to track the evolution of the free surface. The volume fraction value for each element varies from zero to one, where zero denotes an empty or void element and one denotes a full or fluid element. The values between zero and one indicate that the corresponding elements are the partially full or surface elements, and the free surface can thus be determined by the distribution of the volume fraction. ALE is a numerical method to enable grid deformations and avoid elements from large deformation in solution procedures.

Fig. 3 illustrates the mesh layout of FEM simulation, where gray elements correspond to polymer flow (volume fraction = 1.0, means flow occupied with

element), and the white elements relate to air (volume fraction = 0.0) in initial condition with DR = 0.5, TR = 1.

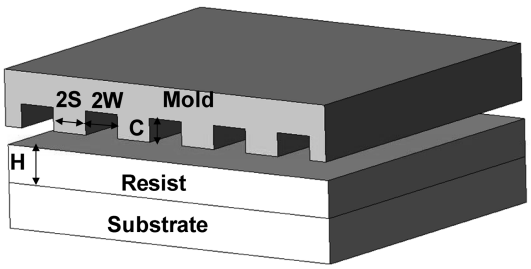

Fig. 1. Geometrical definition for NIL.

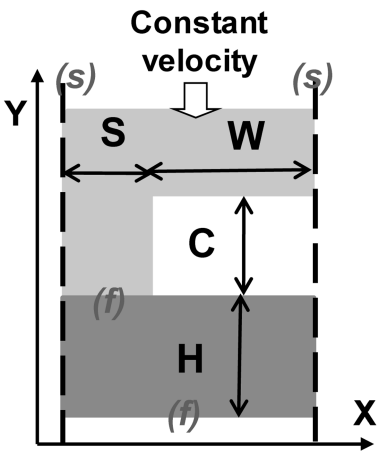

Fig. 2. Computation domain (a unit cell of symmetric and regular line-and-space pattern) and boundary condition; *(f)* represents non-slip boundary conditions and *(s)* indicates symmetric boundary conditions.

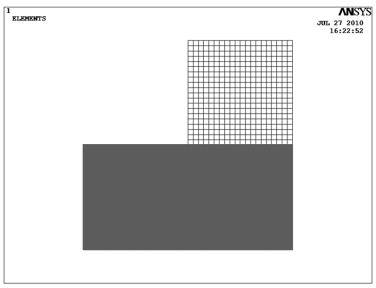

Fig. 3. FEM model in initial condition where gray elements correspond to polymer flow, and the white elements relate to air.

3. Results and Discussions

Fig. 4 shows the simulated free surface shapes of the PMMA resist with 3 different filling ratios, 0.2, 0.5 and 0.8, under the process conditions of constant velocity V=50 nm/s, and the mold shape of W= 250 nm, S=250nm, C=250nm, H=250nm, DR=0.5, TR=1. The surface tension and gravity effect are considered and the value of surface tension considered is 29.7 mN/m. All the free surface shapes considered show single peak and cavity center to be convex, which means that the polymer resist flow reaches the top surface of the mold cavity.

Fig. 5 shows the simulation results of velocity vector distributions and pressure distributions at various filling ratios under the same conditions shown in Fig. 4. Fig. 5 (a), (c) and (e) show respectively polymer flow characteristics at filling ratio, FR=0.2, 0.5 and 0.8. The polymer material underneath mold teeth squeezed by the mold results the flow in Y direction movement. The flow gradually turns into X direction and then advance forward to cavity center. After that, the flow keeps going upwards to fill the cavity until it touches the top surface of the mold cavity. At filling ratio, FR=0.8, the polymer flow is seen to touch the mold and the mold enforces flow downward and sideward to fill the corner of mold cavity. The flow near the mold teeth corner shows smaller radius of curvature. Smaller radius of curvature for the velocity vector distributions means higher velocity gradient. Since the shear stress of Newtonian viscous flow is linearly proportional to the velocity gradient, smaller radius of curvature will induce larger pressure at that location. Fig. 5 (b), (d) and (f) show respectively polymer pressure characteristics at filling ratio, FR=0.2, 0.5 and 0.8. The polymer material underneath mold teeth squeezed by the mold has uniform and large pressure distribution. The correspondence of smaller radius of curvature for the velocity vector distributions with larger pressure value for the pressure distributions can be observed in Fig. 5 (a)-(b), (c)-(d) and (e)-(f).

Fig. 6 presents the imprinting pressure evolution with respect to filling ratio during the imprinting process under the conditions described previously. At early stage, a little pressure is necessary for the imprinting process. Afterwards, pressure grows slightly and then increases steeply after about FR=

0.8, which is also explained by the squeeze flow theory where a squeezing pressure is in inverse proportion to the third power of a thickness of the resist thickness [12].

In order to investigate the effects of initial resist thickness on polymer flow field during thermal NIL, the simulations were performed under the same conditions shown in Fig. 4 only changing the initial resist thickness or TR parameter: H=125nm, 250nm, 500nm or TR=0.5, 1.0, 2.0. Fig. 7 shows numerical results of free surface shapes with the filling ratio increasing and it can be seen that the change of initial resist thickness has little effect on the free surface shapes in thermal NIL. In the case of the imprinting pressure required for the constant imprinting velocity, however, it was shown that as the initial resist thickness decreases, the imprinting pressure required for the constant imprinting velocity increases steeply as shown in Fig. 8, which qualitatively matched the squeeze flow theory.

Let's investigate the effect of different mold shapes (different DR) on polymer flow field during thermal NIL. Fig. 9 shows numerical results of free surface shapes under the conditions of the DR changes

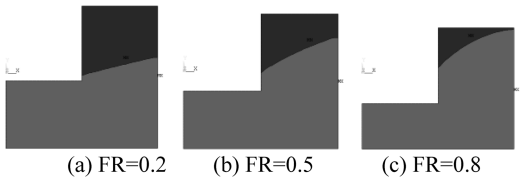

Fig. 4. Free surface shapes at various filling rates under the conditions of V=50 nm/s, DR=0.5, TR=1.

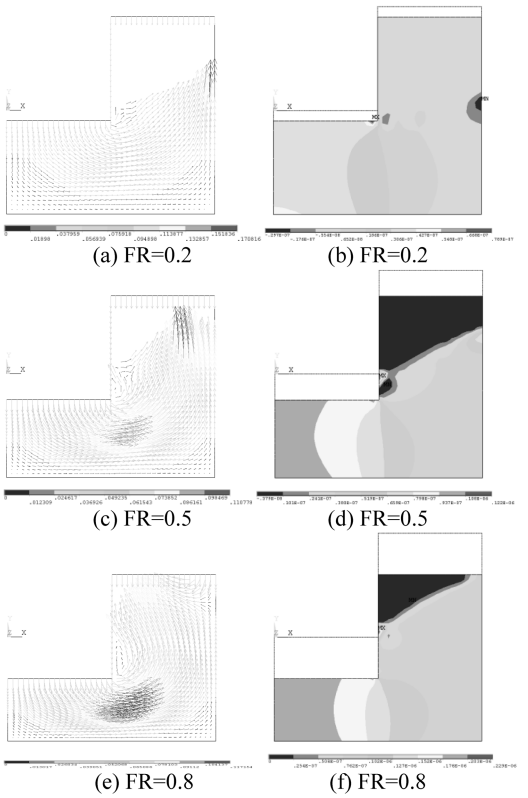

Fig. 5. Velocity vector and pressure distributions at various filling ratios under the same conditions shown in Fig. 4.

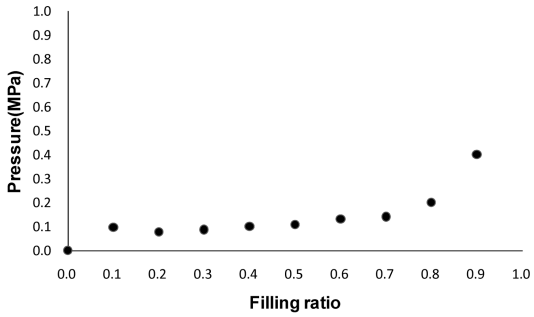

Fig. 6. Imprinting pressure evolution with respect to filling ratio.

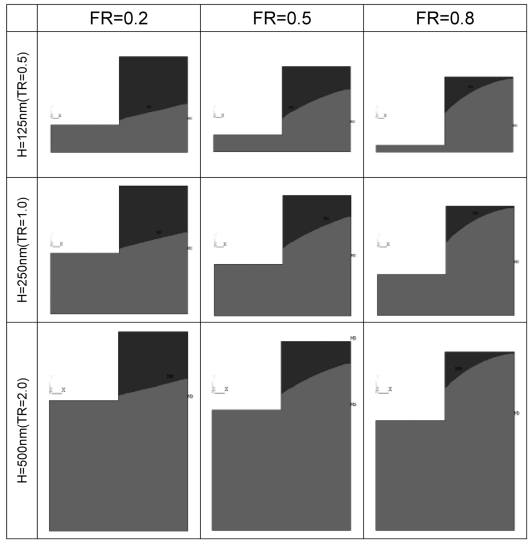

Fig. 7. Free surface shapes under the conditions of V=50 nm/s, DR=0.5 and TR=0.5, 1.0, 2.0.

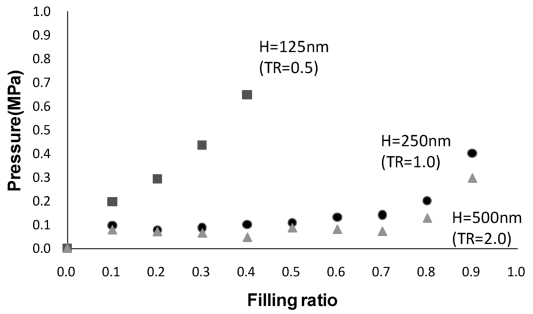

Fig. 8. Pressure evolution with respect to filling ratio for various TRs.

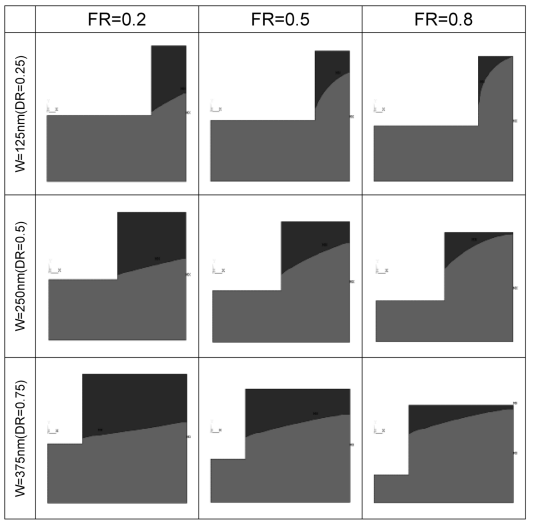

Fig. 9. Free surface shapes under the conditions of V=50 nm/s, TR=1.0 and DR=0.25, 0.50, 0.75.

(DR=0.25(W=125 nm, S=375 nm), DR=0.5(W=250 nm, S=250 nm), DR=0.75 (W=0.375 nm, S=0.125 nm)) with the filling ratio increasing. It can be seen that as the DR increases, the convexity of the free surface in the mold cavity decreases, which is depicted by other researches [7, 8]. Fig. 10 shows pressure required for the constant imprinting velocity under the conditions of the DR changes. The change of DR results in the change of the imprinting pressure and the relation between imprinting pressure and duty ratio has a tendency to be in inverse proportion.

4. Conclusions

In order to understand polymer flow phenomena in thermal NIL, a numerical analysis using a commercial FEM code, ANSYS, was carried out. From the simulation, the following conclusions can be drawn.

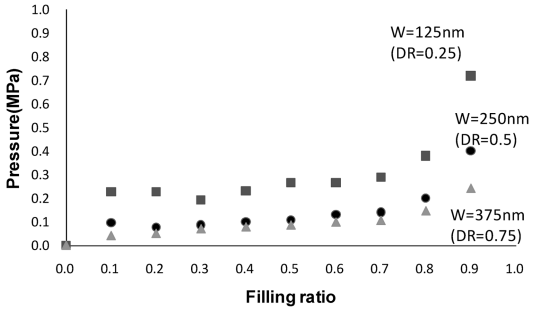

Fig. 10. Pressure evolution with respect to filling ratio for various DRs.

1. From the simulated velocity fields of polymer flow, the mechanism of nanoimprint forming such as free surface shape, velocity vector distribution and pressure distribution, and the imprinting pressure required for the constant imprinting velocity were obtained.

2. The investigation of effects of initial resist thickness on polymer flow shows that the change of initial resist thickness has little effect on the free surface shapes but has a big impact on the imprinting pressure for constant imprinting velocity, which qualitatively matched the squeeze flow theory.

3. From the simulation of effects of different mold shapes (change of duty ratio) on polymer flow, it can be seen that as the duty ratio increases, the convexity of the free surface in the mold cavity decreases and the imprinting pressure for constant imprinting velocity also decreases.

References

1. Chou, S. and Krauss, P., "Imprint lithography with sub-10nm feature size and high throughput," Microelectronic Engineering., Vol. 35, pp. 237-240, 1997.
2. Guo, L.J., "Recent progress in nanoimprint technology and its applications," Journal of Physics. D: Appl. Phys., Vol. 37, pp. R123-R141, 2004.
3. Hirai, T., Fujiwara, M., Okuno, T., Tanaka, Y., Endo, M., Irie, S., Nakagawa, K. and Sasago, M., "Study of the resist deformation in nanoimprint lithography", Journal of Vacuum Science and Technology B, Vol.

19, pp. 2811-2815, 2001.
4. Hirai, Y., Konish, T., Yoshikawa, T. and Yoshida, S., "Simulation and experimental study of polymer deformation in nanoimprint lithography", Journal of Vaccum Science and Technology B, Vol. 22, pp. 3288-3293, 2004.
5. Kim, N.W., Kim, K.W., and Sin, H.-C., "Finite element analysis of low temperature thermal nanoimprint lithography using a viscoelastic model," Microelectronic Engineering., Vol. 85, pp. 1858-1865, 2008.
6. Jeong, J.-H., Choi, Y.-S., Shin, Y.-J., Lee, J.-J. and Park, K.T., "Flow behavior at the embossing stage of nanoimprint lithography", Fibers and Polymers, Vol. 3, pp. 113-119, 2002.
7. Lee, Y.H., Kim, N.W. and Sin, H.-C., "Effect of boundary slip phenomena in nanoimprint lithography process", Transaction of the Korean Society of Machine Tool Engineer, Vol. 18, pp. 144-153, 2009.
8. Rowland, H.D. and King, W.P., "Polymer deformation and filling modes during microembossing", Journal of Micromechanics and Microengineering, Vol. 14, pp. 1625-1632, 2004.
9. Son, J.-W., Song, N.-H., Rhim, S.-H. and Oh, S.-I., "Prediction of Defects in Nano-Imprint Lithography Using FEM Simulation", Key Engineering Materials, Vol. 345-346, pp. 665-668, 2007.
10. Song, J.H., Huh, H., Kim, S.H. and Hahn, H.T., "Finite Element Analysis of Room Temperature Nanoimprint Lithography Process with Rate Dependent Plasticity", Material Science Forum, Vol. 85, pp. 505-507, 2006.
11. Schift, H., Heyderman, L.J., in: C.M. Sotomayor Torres (Ed.), Alternative Lithography, Kluwer Academic/Plenum, 2003.
12. Kim, N. W., Kim, K. W., and Sin, H.-C., "A mathematical model for slip phenomenon in a cavity-filling process of nanoimprint lithography," Microelectronic Engineering., Vol. 86, pp. 2324-2329, 2009.

접수일: 2010년 8월 16일, 심사일: 2010년 8월 27일,
게재확정일: 2010년 9월 15일